CHEMISTRY OF MATERIALS
Article

Chem. Mater. **2009,** *21,* 4631–4637 4631
DOI:10.1021/cm901694r

Nanostructured Photovoltaic Devices from Thermally-Reactive π-Conjugated Polymer Blends

Xu Han,[†] Xiwen Chen,[‡] and Steven Holdcroft*

Department of Chemistry, Simon Fraser University, Burnaby, British Columbia, Canada V5A 1S6. [†]*Current address: Department of Materials Science and Engineering, Stanford University, Palo Alto, CA 94305.* [‡]*Current address: Flexible Electronics, Future Manufacturing Flagship, CSIRO Molecular and Health Technologies, Clayton, Victoria 3168, Australia.*

Received June 18, 2009. Revised Manuscript Received August 21, 2009

A facile method for preparing nano- and microstructured π-conjugated polymers (πCPs) from polymers bearing thermally cleavable solubilizing groups for the application of organic photovoltaic cells is described. Solutions of thermally reactive poly[3-(2-(2-tetrahydropyranyloxy)ethyl)thiophene)] (PTHPET), poly(methylmethacrylate) (PMMA), and camphorsulfonic acid were spin-cast to yield nano- and micro- phase segregated thin films, ~100 nm thick. A thermally induced, acid-catalyzed, solid-phase reaction, in which the tetrahydropyran group is eliminated, renders the conjugated polymer insoluble. Subsequent removal of PMMA by dissolution affords retention of the conjugated polymer in the form of nano/microarchitectures. This strategy proved useful in the fabrication of controlled nano/microscale structures for organic photovoltaic cells devices, wherein insoluble, nanostructured De-PTHPET served as a donor layer and a spin-cast solution of PCBM accessed the recesses of the film to serve as the electron acceptor layer. The properties of nanopatterned PV devices are compared to conventional bilayer, and bulk heterojunction devices. The nanostructured, donor−acceptor films provided an advantage over molecularly blended films in that potential isolation of electron acceptor in the donor film is decreased, and vice versa, mitigating charge trapping, and providing improved device efficiency.

Introduction

π-Conjugated polymers (πCPs) are attractive materials because of their application in organic electronic devices such as polymer light-emitting displays,[1] photovoltaic panels,[2] and field-effect transistors.[3] An emerging subgroup of this class of material are thermally reactive πCPs, which are πCPs that bear thermally cleavable groups such as a carboxylic acid esters or tetrahydropyran (THP). These groups can be homolytically cleaved and volatilized at elevated temperature from thin films, or catalytically at lower temperature, to yield the corresponding deprotected π-conjugated polymer, which is often insoluble in common solvents. Yu et al. report the synthesis of several regioregular polythiophenes bearing the 2-tetrahydropyranyl (THP) group which homolytically cleaves between 200 and 300 °C in the solid state, but catalytically at much lower temperature, e.g., ~130 °C, in the presence of trace of acid.[4] The acid-catalyzed elimination of dihydropyran from poly[3-(2-(2-tetrahydropyranyloxy)-ethyl)thiophene)] (PTHPET) is illustrated in Scheme 1.

Thermally reactive polymers are currently being investigated as process-facilitating materials in the fabrication of photovoltaic devices. Liu et al. report the synthesis of a thermocleavable carboxylic acid ester attached to polythiophene, poly-(3-(2-methylhexan-2-yl)-oxy-carbonyldithiophene) (P3MHOCT), which served as an interfacial layer between a TiO_2 electrode and poly-3-hexylthiophene (P3-HT) photoactive layer.[5] The ester groups, which render the polymer solution processable, can be eliminated by heating to ~200 °C to yield poly-3-carboxydithiophene (P3CT). A hybrid solar cell device containing a layer of P3CT yields a 3-fold increase in photocurrent compared to a device prepared without. Krebs et al. report that P3CT may be used to yield solar cells possessing lifetimes in excess of 10 000 h under AM 1.5D illumination at elevated temperatures under oxygen and moisture free environments.[6] Recently, it was reported that P3CT can be decarboxylated to polythiophene (PT) upon heating at ~300 °C.[7] Efficiencies up to 1.5% are reported for bulk heterojunctions based on these materials in combination with [6,6]-phenyl-C_{71}-butyric acid methyl ester ([70]PCBM). More recently, Krebs et al. report a new series of thermocleavable esters of low band gap polymers based on diphenyldithienylthienopyrazine and PV power conversion efficiencies of

*To whom correspondence should be addressed. Fax: (604) 291-3765. E-mail: holdcrof@sfu.ca.

(1) Burrows, P. E.; Gu, G.; Bulovic, V.; Shen, Z.; Forrest, S. R.; Thompson, M. E. *IEEE Trans. Electron Devices* **1997**, *44*, 1188.
(2) Winder, C.; Sariciftci, N. S. *J. Mater. Chem.* **2004**, *14*, 1077.
(3) Stutzmann, N.; Friend, R. H.; Sirringhaus, H. *Science* **2003**, *299*, 1881.
(4) (a) Yu, J.; Holdcroft, S. *Macromolecules* **2000**, *33*, 5073. (b) Yu, J.; Abley, M.; Yang, C.; Holdcroft, S. *Chem. Commun.* **1998**, 1503. (c) Yu, J.; Holdcroft, S. *Chem. Mater.* **2002**, *14*, 3705. (d) Yu, J.; Holdcroft, S. *Chem. Mater.* **2001**, *13*, 526.
(5) Liu, J. S.; Kadnikova, E. N.; Liu, Y. X.; McGehee, M. D.; Fréchet, J. M. J. *J. Am. Chem. Soc.* **2004**, *126*, 9486.
(6) Krebs, F. C. *Proc. SPIE* **2005**, *5938*, 59380Y.
(7) Gevorgyan, S. A.; Krebs, F. C. *Chem. Mater.* **2008**, *20*, 4386.

Published on Web 09/17/2009

Scheme 1. Acid-Catalyzed Elimination of Dihydropyran from PTHPET

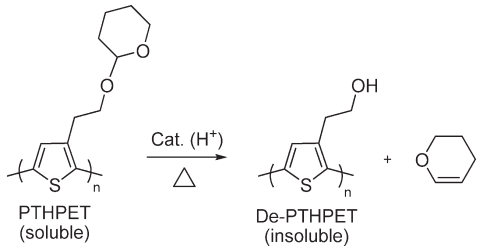

0.4% for ITO/poly-3,4-ethylenedioxythiophene polystyrenesulfonate (PEDOT-PSS)/polymer-/PCBM/Al devices.[8]

The photovoltaic power-generating process includes photon absorption, exciton creation, diffusion and dissociation, carrier separation and transport, and charge collection.[9] Single layer and bilayer heterojunction organic PV devices exhibit relatively low solar efficiencies compared to their inorganic counterparts partly because of the limited exciton diffusion length, short minority carrier lifetimes, and large electrical resistance of organic films.[10] The bulk heterojunction has proved the most efficient morphological film architecture to date for polymeric PV devices because exciton harvesting is enhanced.[11] However, the random distribution of electron acceptor molecules within a film of a polymeric electron donor can lead to electron trapping within isolated domains of acceptors and a reduction in purity of the donor and acceptor phases. This challenge—enhancing the purity of the two domains, while maintaining a high interfacial area and bicontinuity—has inspired the investigation of highly ordered morphological architectures. These include the use of TiO_2-hybrid structures[12] and block copolymer films.[13] The requirements for high efficiency also dictate that both donor and acceptor domains have short pathways to the electrode in order to facilitate carrier transport to adjacent electrodes. Moreover, each phase of the heterojunction should be in contact with only one of the electrodes in order to maintain a high shunt resistance and minimization of carrier losses. Also, to obtain long-term device performance, morphological stability at elevated temperatures is required. Hence there is current interest in the incorporation of compatibilizers to control phase segregation in donor/ acceptor blends,[14] and in thermally reactive polymers to "lock-in" polymer morphology.[6−8]

In a previous report, we described an approach to the formation of morphologically controlled nano/microscale patterns of πCPs by spin-casting acidic, binary polymer solutions of polythiophene−bearing a thermally cleavable solubilizing group−and PMMA.[15] Phase segregation of πCP/PMMA, induced by the chemical dissimilarity of the two polymers, resulted in films exhibiting a nano/micropatterned morphology. Elimination of thermally labile groups renders the resulting πCP insoluble and removal of the PMMA by dissolution leaves a dot matrix of conjugated polymer. In this paper, we address a proof-of-concept strategy that involves phase segregation of donor/acceptor blends and thermally reactive polymers that "lock-in" the polymer morphology. Here, we use nano/microsized πCP domains onto which a layer of PCBM is spin-cast to fabricate PV devices as illustrated in Figure 1. To investigate the role of the morphological architecture of the photoactive material, we compared PV devices fabricated using patterned πCP/PCBM films to devices fabricated using conventional πCP/PCBM bulk heterojunction blends and bilayers.

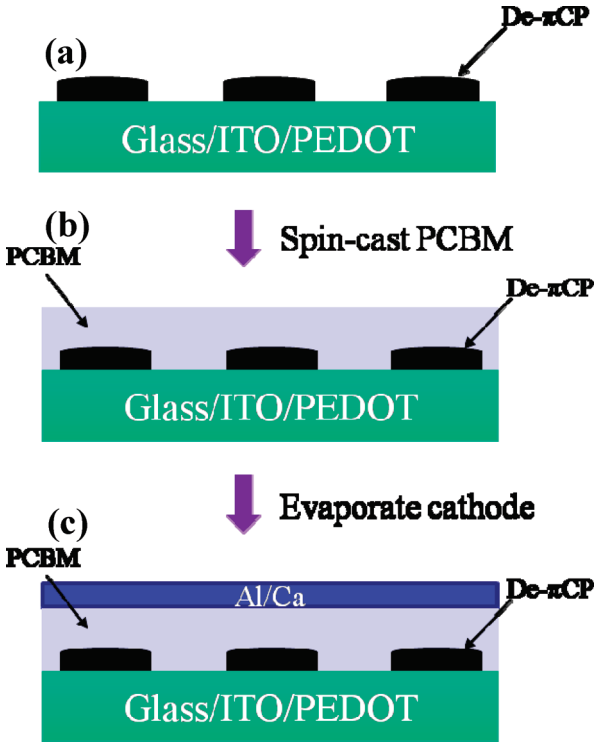

Figure 1. Schematic Illustration of the Fabrication of Nano/Micropatterned, Donor−Acceptor PV Devices.

Experimental Section

Materials. Poly(methyl methacrylate) (PMMA) (M_n = 48,300 Da), camphorsulfonic acid (CSA), Ni(dppp)Cl_2, methylmagnesium bromide, chlorobenzene, chloroform, methanol, hexanes, and THF were purchased from Aldrich and used as-received. [6,6]-Phenyl C_{61} butyric acid methyl ester (PCBM) was purchased from American Dye Source, Inc. and used as received. Regioregular PTHPET was synthesized using the Grignard metathesis (GRIM) method.[15]

Synthesis of PTHPET (Scheme 2). 2,5-Dibromo-3-(2-(2-tetrahydropyranyl-2-oxy)ethyl)thiophene (diBrTHPET) (2.56 g, 6.90 mmol) was dissolved in 40 mL of dry THF. Methylmagnesium bromide (6.9 mL, 1.0 M solution in butyl ether) was added and the mixture was heated to reflux for 1 h. Ni(dppp)Cl_2 (36 mg) was added and

(8) Petersen, M. H.; Gevorgyan, S. A.; Krebs, F. C. *Macromolecules* **2008**, *41*, 8986.
(9) Bube, R. H. In *Photovoltaic Material*; Imperial College Press: London, 1998; pp 2 and 219.
(10) Hoppe, H.; Sariciftci, N. S. *J. Mater. Res.* **2004**, *19*, 1924.
(11) Dennler, G.; Scharber, M. C.; Brabec, C. *J. Adv. Mater.* **2009**, *21*, 1.
(12) Coakley, K. M.; McGehee, M. D. *Chem. Mater.* **2004**, *16*, 4533.
(13) (a) Scherf, U.; Gutacker, A.; Koenen, N. *Acc. Chem. Res.* **2008**, *41*, 1086. (b) Chen, X.; Gholamkhass, B.; Han, X.; Vamvounis, G.; Holdcroft, S. *Macromol. Rapid Commun.* **2007**, *28*, 1792.
(14) Sivula, K.; Ball, Z. T.; Watanabe, N.; Fréchet, J. M. *J. Adv. Mater.* **2006**, *18*, 206.
(15) Han, X.; Chen, X.; Holdcroft, S. *Adv. Mater.* **2007**, *19*, 1697.
(16) Loewe, R. S.; Khersonsky, S. M.; McCullough, R. D. *Adv. Mater.* **1999**, *11*, 250.

Scheme 2. Synthesis of Thermally-Reactive π-Conjugated Polymer PTHPET

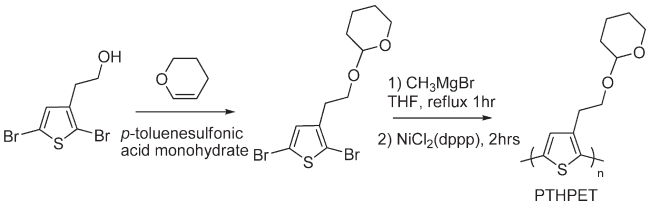

the solution stirred at reflux for 2 h. The mixture was poured into 300 mL of methanol and filtered through a Soxhlet thimble. Soxhlet extractions were performed with methanol (to remove monomer and salts), hexanes (to remove catalyst and oligomers), and chloroform. The chloroform fraction was reduced in volume and product dried in a vacuum to afford 1.11 g (76% yield) of the title polymer. ^{1}H NMR: (500 MHz, CD_2Cl_2) δ 7.19 (s, 1H, aromatic region), 4.64 (s, 1H), 4.03−3.45 (m, 4H,), 3.11 (t, 2H), 1.83−1.1.51 (m, 6H). M_n = 22 700 Da, PDI = 1.68.

Blends of PTHPET/PMMA (30:70, 40:60, 50:50, 60:40, and 70:30 wt %) were prepared by casting chlorobenzene/THF (95:5 vol%) solutions (12 mg/mL). Solutions contained 5 mol % camphorsulfonic acid (based on mole percent of THP present). All solutions were mixed ultrasonically for 5 min and filtered (0.2 μm pore size) prior to spin-casting onto glass or silicon wafers at 1500 rpm for 90 s. The resultant films were dried overnight under vacuum to remove residual solvent. Acid-catalyzed deprotection of the films was carried out by heating at ~150 °C for 3 min. Deprotected films were developed by rinsing with chlorobenzene/hexane (50:50 vol%).

Measurements. 500 MHz ^{1}H and 125 MHz ^{13}C NMR spectra were obtained in CD_2Cl_2 on a Varian AS500 spectrometer; chemical shifts are reported in parts per million (ppm), referenced to CD_2Cl_2 (^{1}H: δ = 5.32 (t); ^{13}C: δ = 54.00 (quintet)). Molecular weights were estimated by gel permeation chromatography (GPC) (Waters model 1515 isocratic pump) equipped with μ-Styragel columns referenced to polystyrene standards. Polymers were eluted with THF using a flow rate of 1.0 mL/min and detected with a UV−vis detector (Waters model 2487) at 254 nm. Atomic force microscopy (AFM) was performed with an Explorer AFM system (Thermomicroscopes, Sunnyvale, CA) and SPMLabNT software, version 5.01 Explorer AFM, operated in the tapping mode. Thermogravimetric analyses (TGA) were performed at 10 °C/min on 3−5 mg of polymer sample under N_2 using a HiRes TGA 2950 Thermogravimetric Analyzer (TA Instruments). The onset temperature of deprotection was estimated from the point of intersection of two lines: one extrapolated from the slope of the curve just prior to loss of the THP group and the second from the inflection point. Mass loss was obtained with ±1% error. UV−vis absorption spectra were recorded on a Cary 300 Bio (Varian) spectrophotometer.

Device Fabrication and Characterization. PTHPET/PCBM bulk heterojunction (BHJ) PV devices were fabricated according to the following procedure: indium−tin oxide (ITO) glass (sheet resistance 20 Ω/sq., Merck Display Technologies Ltd., Taiwan) was patterned and cleaned in a sonicating bath consecutively with deionized water, acetone, isopropanol, and hexane. A layer of poly(styrene sulfonic acid)-doped poly(ethylenedioxythiophene) (PEDOT:PSS, 1.5 wt %, AI4083, from H. C. Starck.) (~30 nm) was spin-cast at 5000 rpm from aqueous dispersion (after passing through a 0.45 μm filter) on top of ITO glass, and heated at 140 °C for 10 min. The substrate was transferred to a N_2-filled glovebox (< 0.1 ppm O_2 and H_2O) for spin-casting the photoactive layer. Solutions of polymers blended with PCBM (e.g., 10.0 mg of PTHPET and 20.0 mg of PCBM in 1.0 mL chlorobenzene) were spin-cast on top of PEDOT at 700 rpm for 60s to produce ~120 nm thick films, as determined by profilometry (KLA Tencor). A layer of calcium (~25 nm), followed by a layer of aluminum (~100 nm), was thermally deposited in a vacuum chamber (~2 × 10^{-6} Torr) through a shadow mask, which had a defined active area of ~0.10 cm^2. Photovoltaic cells were placed in a custom-built holder and subjected to vacuum prior to PV measurements.

PTHPET/PCBM bilayer PV devices were fabricated according to the procedure above for bulk heterojunction PV devices except for the preparation of the photoactive layer: PTHPET layers were prepared by casting chlorobenzene/THF (95:5 vol%) solutions of the polymer (10.0 mg/mL). Solutions contained 5 mol % camphorsulfonic acid. All solutions were spin-cast at 700 rpm for 60s on top of the PEDOT:PSS layer. Acid-catalyzed deprotection of the films was carried out by heating the samples for 3 min at ~150 °C. Deprotected films were rinsed with chlorobenzene/hexane (50:50 vol%). A layer of PCBM was spin-cast at 700 rpm for 60s on top of the deprotected layer using a 20 mg/mL chlorobenzene solution. The combined thickness of the films was ~90 nm as measured by profilometry (KLA Tencor).

PTHPET/PCBM nanopatterned PV devices were fabricated according to the procedure above for bulk heterojunction PV devices except for the preparation of the photoactive layer: blends of PTHPET/PMMA (40:60 wt %) were prepared by casting chlorobenzene/THF (95:5 vol%) solutions of the polymers (25.0 mg/mL). Solutions contained 5 mol % camphorsulfonic acid. All solutions were spin-cast at 700 rpm for 60s on top of the PEDOT:PSS layer. Acid-catalyzed deprotection of the films was carried out by heating the samples for 3 min at ~150 °C. Deprotected films were developed and patterned by rinsing with chlorobenzene/hexane (50:50 vol%). PCBM was spin-cast at 700 rpm for 60s on the patterned De-PTHPET layer from a 20 mg/mL chlorobenzene solution. The combined thickness of the films was ~130 nm as measured by profilometry.

Current−voltage characteristics of the PV devices were measured using a Keithley 2400 source meter under illumination with an ozone-free Xenon 500 W lamp through an AM 1.5D filter (Newport Co.). The power was adjusted to 100 mW/cm^2, as measured by a calibrated Radiant Power Meter (model 70260) combined with a 70268 probe. The measurements of device performance were performed several times on each device. The incident photon-to-current collection efficiency (IPCE) spectrum was determined by measuring the PV current generated upon exposure to monochromatic light emerging from an Oriel Cornerstone 260 1/4 m monochromator/Xenon 500 W lamp system. The incident light intensity of monochromatic light was measured with a Newport optical power and energy meter (model 841-PE) equipped with a model 818-UV low power detector. The internal quantum efficiency (IQE), given by the average number of electrons generated per photon absorbed, was estimated from IQE = EQE/Abs = EQE/(1 − T − R), where Abs is the absorbance, T is the transmittance, and R is the reflectance. T was calculated using Beer's law $T = 10^{-A}$, where A is optical absorbance. R is estimated from the ratio of incident light intensity in the presence and absence of ITO-coated glass. R was ~0.2 at 435 nm.

Results and Discussion

The synthesis of regioregular PTHPET using the GRIM Method is shown in Scheme 2. ^{1}H NMR spectroscopic

analysis confirmed the molecular structure of the polymer. The resonance peaks at 7.19 and 4.64 ppm are assigned to the aromatic protons of the thiophene ring and methine of THP, respectively. The molecular weight (M_n = 22 700 Da) and polydispersity index (PDI = 1.68) of PTHPET are typical of thiophene-based polymers prepared by the GRIM reaction. TGA thermograms of PTHPET were carried out in the absence and in the presence of CSA, and are shown in Figure 2. The observed weight loss values of 35 wt % in the absence of acid and 38 wt % in the presence of acid are consistent with the theoretical loss in mass (40 wt %) due to thermolytic cleavage of the THP group and elimination of dihydropyran. The onset temperature required to remove the THP group from PTHPET is 230 °C in the absence of acid and 130 °C in the presence of acid, similar to the onset temperature previously reported for similar polymers.[4b]

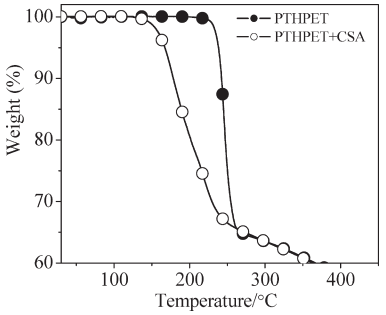

Figure 2. TGA thermograms of PTHPET in the absence and presence of camphorsulfonic acid (CSA).

A schematic diagram illustrating the formation of nano/microsized domains of deprotected PTHPET (De-PTHPET) is shown in Figure 3. Significant efforts were made to optimize the solution-casting method, some of which are reported elsewhere.[15] The parameters optimized include selection of the vinylic polymer, solvent, concentration of the polymer blend solution, composition of the blend, spin-casting speed, substrate, and volume of solution applied to the substrate. In this work, PTHPET/PMMA (12 mg/mL in total, 40:60 wt %) in chlorobenzene/THF (95:5 vol%) was spin-cast on a silicon wafer in the presence of a catalytic amount of camphorsulfonic acid (CSA). A binary thin film formed upon solvent evaporation. The thickness of the films was ~100 nm, but the πCP domains are recessed ~50 nm. PMMA forms a continuous phase, of greater thickness, while PTHPET domains occupy the lower half of the film and form disk-like shapes (~500 nm in diameter) that penetrate into the PMMA matrix, as shown in the 3D AFM image Figure 3d. PTHPET domains are recessed with respect to PMMA domains and a fraction of the PTHPET domain is not exposed when viewed top-down. The 3D image exhibits a "Swiss cheese" morphology. The driving force for phase segregation of the polymer blend is the difference in Flory−Huggins interaction parameter of the two dissimilar polymers and their difference in solubility. During spin-casting, the less volatile solvent, chlorobenzene

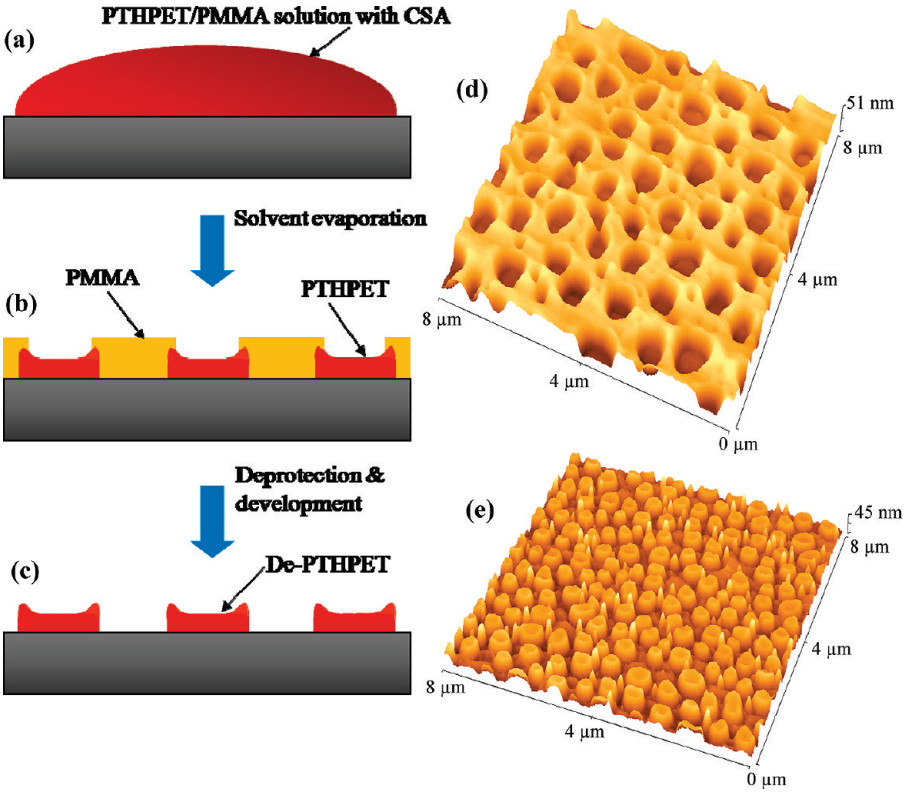

Figure 3. Schematic illustration of the formation of micro/nanosized De-PTHPET features by (a) consecutive solution casting, (b) self-organization, and (c) catalytic reaction and development. 3D AFM topographical scans of (d) PTHPET/PMMA (40:60 wt %) blended film (~100 nm thickness) in the presence of acid cast from solution (12 mg/mL) and (e) deprotected film De-PTHPET (~50 nm thickness, ~500 nm sized domains) after dissolution of PMMA.

evaporates slower than THF, thus facilitating demixing of PTHPET and PMMA. As PMMA is less soluble in chlorobenzene than PTHPET, the PMMA phase is more quickly depleted of solvent and begins to solidify. This observation is consistent with previous reports of demixing of binary polymer solutions upon solvent evaporation,[17] which is described in more detail in a previous report.[15] The PTHPET domains are rendered insoluble upon heating the films at 150 °C for 3 min due to acid-catalyzed elimination of THP. Following dissolution of PMMA, disk-shaped domains of De-PTHPET remain, as illustrated in Figure 3c and 3e. The De-PTHPET domains are ~50 nm in thickness and their distribution correlates to that observed in the pristine, undeveloped film. The discs are slightly larger in diameter when developed (~500 nm) than observed in Figure 3c because recessed πCP domains being partially covered by PMMA.

The dependence of the resultant morphology of the binary films on the composition ratio of PTHPET/PMMA polymer solutions is illustrated in Figure 4. Films of binary composition were spin-cast from polymer solutions (12 mg/mL) having compositions: 30:70, 40:60, 50:50, 60:40, and 70:30 wt % PTHPET/PMMA. AFM topographies of pristine films in the presence of acid are shown in Figure 4a, c, e, g, and i, respectively. The lighter regions represent PMMA domains; the darker regions represent PTHPET domains. AFM topographies of deprotected films, De-PTHPET, after rinsing with chlorobenzene/hexane (50:50 vol%) are shown in Figure 4b, d, f, h, and j, respectively. In these images, the lighter regions represent De-PTHPET domains; darker regions, the substrate. Decreasing the mass ratio of PMMA in the blend causes the PMMA domains to cover a smaller area, ultimately leading to discontinuous, wormlike phases that possess larger heights than the PTHPET domains. In contrast, as the PMMA content is reduced, the original PTHPET domains, which are scattered as disk-shaped regions 200−500 nm in diameter, increase in size and form a continuous phase. The increase in domain size of the πCP is consistent with the increase of πCP weight ratio in polymer blend solutions; hence the domain size of the πCP may be partially controlled by the blend composition of the casting solution.

In a similar manner, nanopatterned De-PTHPET was deposited on PEDOT:PSS cast onto ITO-coated glass, as the initial step in PV device fabrication. PCBM was spin-cast onto patterned De-PTHPET from a 20 mg/mL chlorobenzene solution, onto which layers of Ca and Al were evaporated. For comparison PTHPET/PCBM bulk heterojunction (BHJ), and PTHPET/PCBM bilayer PV devices were fabricated. Each device was prepared from 10 mg/mL PTHPET and 20 mg/mL PCBM solution according to the described procedure. Figure 5 shows $J-V$ characteristics of the nanopatterned, BHJ, and bilayer PTHPET/PCBM devices under AM 1.5D illumination (100 mW/cm^2).

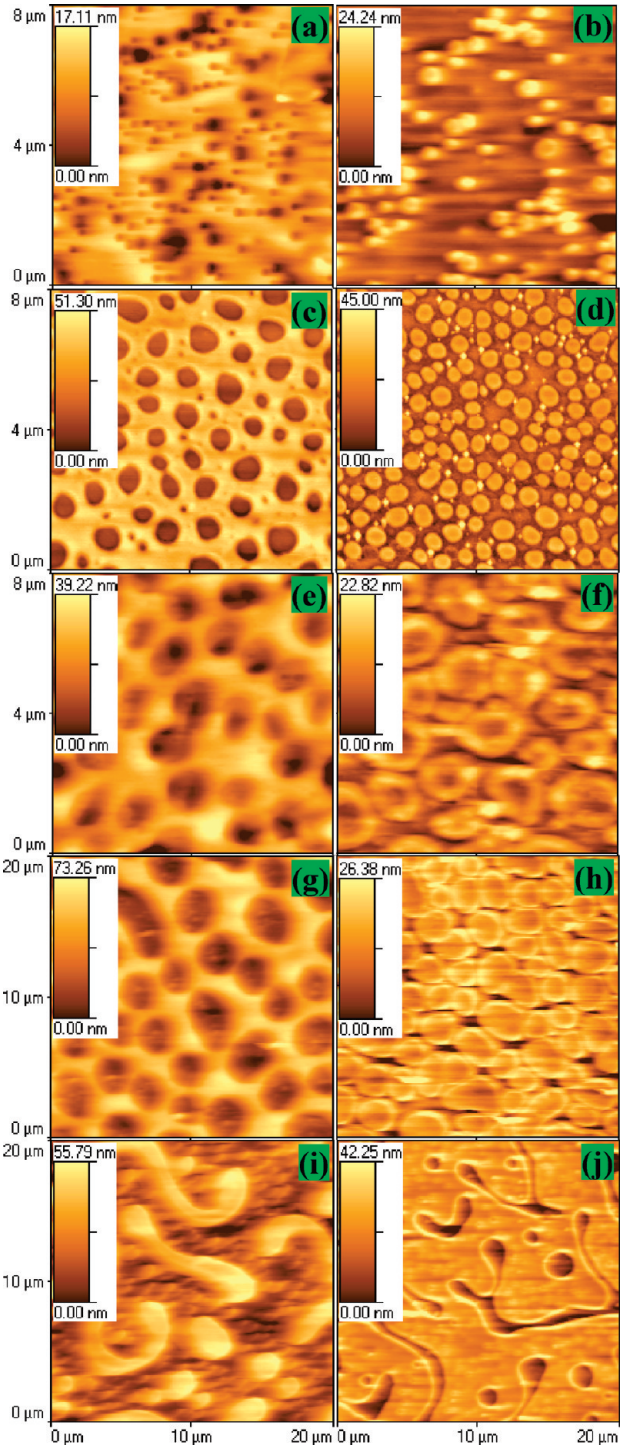

Figure 4. AFM images of PTHPET/PMMA blended films prepared from various mass ratios cast from 12 mg/mL solutions. Pristine films: (a) 30:70, (c) 40:60, (e) 50:50, (g) 60:40, and (i) 70:30 wt %. Corresponding films after deprotection and development: (b) 30:70, (d) 40:60, (f) 50:50, (h) 60:40, and (j) 70:30 wt %.

The device performance, UV−vis absorbance, and transmittance of these devices are summarized in Table 1. The nanopatterned device exhibits $V_{oc} = 0.63$ V, fill factor (FF) = 51.5%, and short circuit current, $J_{sc} = 1.67$ mA/cm^2. The PCE is the highest value of the device series studied (0.54%). The BHJ device (BHJ 1) shows a moderate performance: $V_{oc} = 0.49$ V, $J_{sc} = 1.34$ mA/cm^2, FF = 30.6%, and PCE = 0.2%. The low PCE, compared to current state-of-the-art

(17) Toh-That, C.; Shard, A. G.; Teare, D. O. H.; Bradley, R. H. *Polymer* **2001**, *42*, 1121.

Table 1. PV Device Performance, UV−vis Absorbance, and Transmittance for BHJ 1, Bilayer, Nanopatterned PTHPET, and BHJ 2 (PTHPET 15 mg/mL, PCBM 15 mg/mL) PV Devices

device	J_{sc} (mA/cm^2)	V_{oc} (V)	FF (%)	PCE (%)[d]	EQE* (%)[e]	IQE* (%)[f]	A[g]	T[h]
nanopatterned[a]	1.67	0.63	51.5	0.54	12.4	24.8	0.52	0.30
bilayer[2]	0.58	0.43	45.6	0.11	4.9	9.6	0.54	0.29
BHJ1[b]	1.34	0.49	30.6	0.20	10.3	26.2	0.39	0.41
BHJ2[c]	0.60	0.74	27.7	0.12	6.2	17.8	0.45	0.35

[a] Cast consecutively from 10 mg/mL PTHPET; 20 mg/mL PCBM. [b] Cast from 10 mg/mL PTHPET + 20 mg/mL PCBM. [c] Cast from 15 mg/mL PTHPET + 15 mg/mL PCBM. [d] Photoconversion efficiency, AM 1.5D illumination, 100 mW/cm^2. [e] External quantum efficiency at 435 nm. [f] Internal quantum efficiency (absorbed photons to current) at 435 nm. [g] Absorbance at 435 nm. [h] Transmittance at 435 nm, after correction for reflection.

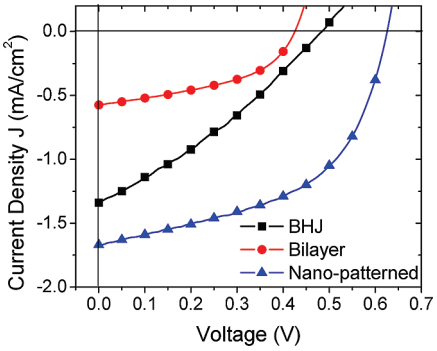

Figure 5. $J-V$ curves obtained from nanopatterned, bulk heterojunction (BHJ1), and bilayer PV devices under 100 mW/cm^2 AM 1.5D illumination.

P3HT/PCBM devices are due to the inherent nature of PTHPET and De-PTHPET, which exhibits a lower degree of coplanarity of individual chains, lower crystallinity of aggregates, lower charge mobility, and blue-shifted absorption spectrum compared to P3HT.[4] When the PTHPET-based BHJ devices were heated to 150 °C (in the presence of acid)−so as to deprotect the PTHPET−the performance of the PV devices fell to negligible values.

The bilayer device exhibits a lower PCE than both the patterned device and the BHJ devices, exhibiting V_{oc} = 0.43 V, J_{sc} = 0.58 mA/cm^2, FF = 45.6%, and PCE = 0.11%. The low J_{sc} and PCE is consistent with bilayer devices,[18] which are limited in donor/ acceptor interfacial area, and because excitons formed outside the exciton diffusion length cannot be dissociated at the interface.

Closer examination reveals that the FF for the nanopatterned device is substantially larger than the BHJ1 device. Low fill factors are often observed when photogenerated charges are trapped with the film or the donor and/or acceptor domains exhibit high resistance to charge transport. The FF of the patterned device is large given the relatively low PCE which indicates that the nanopatterned device morphology offers a favorable donor−acceptor interfacial area, a low extent of trapped charges, and/or an enhanced charge transport pathway for electrons and holes.

UV−vis spectra of PV the active devices prior to deposition of Ca/Al and EQE plots are shown in Figure 6. The photocurrent matches the absorption spectrum of the device. Shown in Table 1 are EQE, IQE, absorbance, and transmittance for these devices at the maximum

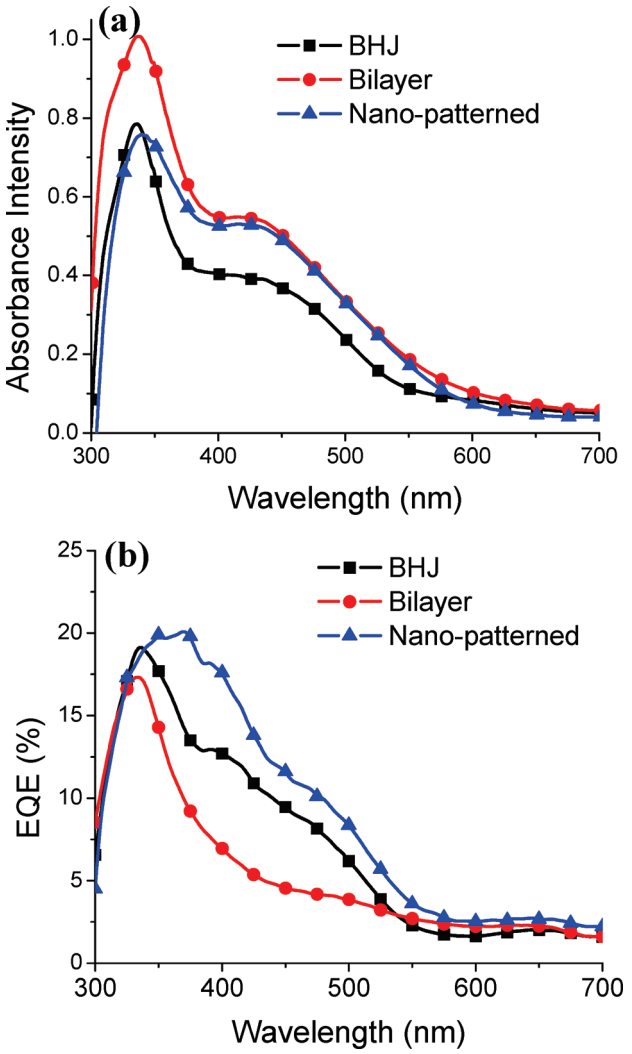

Figure 6. (a) UV−vis absorbance and (b) EQE obtained from nanopatterned, bulk heterojunction (BHJ1), and bilayer PV devices under 100 mW/cm^2 AM 1.5D illumination.

absorption wavelength of PTHPET, i.e., 435 nm. The EQE values are 12.4%, 10.3, and 4.9% at 435 nm for the devices prepared from nanopatterned PTHPET, BHJ1, and bilayers, respectively. The IQE, absorbed photon-to-current efficiencies, estimated from the transmittance, after correcting for reflected light, are 26.2, 24.8, and 9.6%, respectively. The low values for the bilayer device is consistent with the low J_{sc} from these devices and can be explained on the basis that the efficiency of the bilayer device is limited by the exciton diffusion length. The similarity in the IQE values between the nanopatterned

(18) Peumans, P.; Yakimov, A.; Forrest, S. R. *J. Appl. Phys.* **2003**, *93*, 3693.

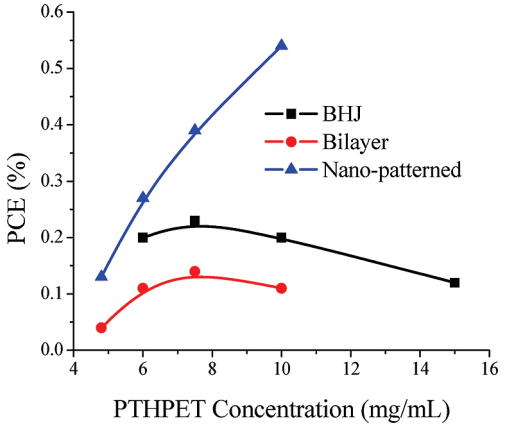

Figure 7. PCE values obtained from nanopatterned, bulk heterojunction, and bilayer PV devices prepared from increasing concentrations of PTHPET, under 100 mW/cm^2 AM 1.5D illumination.

BHJ 1 device deserve further explanation: Spin-casting solutions containing 10 mg/mL PTHPET and 20 mg/mL PCBM solution, in order to prepare BHJ1 films, transfers a substantially lower amount of PTHPET to the substrate than spin-casting films of PTHPET for nanopatterning, because the PTHPET/PCBM solution has a lower viscosity than a solution of PTHPET/PMMA. As result, the BHJ1 device is thinner than nanopatterened films cast from similar solution compositions. This is manifest in their lower absorptivity. Therefore, although the IQEs of the nanopatterned and BH1 devices are similar, 25 and 26%, respectively (because these values are normalized to absorbed photons), the PCE of the BHJ1 is substantially lower (because fewer photons are absorbed). However, increasing the content of PTHPET in the BHJ device, thereby increasing the absorption cross-section, did not improve the PCE, as shown by the PV data obtained from BHJ2. Here, PTHPET was cast from a 15 mg/mL solution so that the absorption of the device was similar to the nanopatterned device. To maintain a BHJ film thickness comparable to BHJ1, the PCBM solution was 15 mg/mL. BHJ2 possessed an absorbance of 0.45 at 435 nm, similar to that of the nanopatterned device ($A = 0.52$). However, the IQE of BHJ2 dropped to 13.9%, much lower than BHJ 1 and nanopatterned devices. Consequently, EQE dropped to 6.2%, which is only a half of that of the nanopatterned device (12.4%), and the PCE was substantially lower.

The effect of the film thickness, as controlled by the concentration of the spin-cast solution is further demonstrated in Figure 7. Nanopatterned devices prepared from PTHPET concentrations of 4.8, 6, 7.5, and 10 mg/mL, which increase the resulting thickness from 70 to 130 nm, show increasing PCE values of 0.13, 0.27, 0.39, and 0.54%. Whereas, bulk heterojunction devices, spin-cast from PTHPET/PCBM solutions (30 mg/mL) having varying weight ratios of 6:24, 7.5:22.5, 10:20, and 15:15; and bilayer devices, cast from increasing concentrations of PTHPET, exhibited lower PCEs. The point of note here is that the thickness of the BHJ and bilayer devices was restricted to relatively thin films. Nanopatterned active layers possess the potential to be prepared much thicker, thus enhancing PCE efficiency.

Conclusion

A simple, solution-based method for preparing nano- and microsized topologies of π-conjugated polymers for PV applications is reported. A unique feature of this work is that the patterned donor layer is rendered insoluble by thermal deprotection enabling an electron-acceptor layer to be sequentially deposited by solution. PV device architectures exhibit a higher power conversion efficiency and larger external quantum efficiency than the corresponding bilayer and bulk heterojunction devices prepared from the same material. This is attributed to the patterned architecture, which improves the donor−acceptor interface, reduces charge trapping, and facilitates a pathway for electrons and holes to reach their respective electrodes.

An area for further research is to improve upon the inherent photoactivity of thermally cleaved PTHPET polymers. Because of their shorter side-chain length and lower semicrystallinity, the inherent charge mobility is much lower than highly photoactive polymers such as P3HT. Furthermore, De-PTHPET possesses a blue-shifted absorption compared to P3HT, for which optimized PV devices can reach in excess of 5% PCE,[19] and therefore is a poor match to the solar spectrum. Increasing the inherent charge mobility, decreasing the domain size, and improving the overlap of with the solar spectrum of nanopatterned πCPs offers a potential strategy for further improvement of polymer-based PV cells.

Acknowledgment. We thank the Natural Sciences and Engineering Research Council of Canada for financial support and Dave Edwards of NRC-IFCI, Vancouver, BC, for thermogravimetric measurements.

(19) (a) Ma, W.; Yang, C.; Gong, X.; Lee, K.; Heeger, A. J. *Adv. Funct. Mater*. **2005**, *15*, 1617. (b) Peet, J.; Kim, J. Y.; Coates, N. E.; Ma, W. L.; Moses, D.; Heeger, A. J.; Bazan, G. C. *Nat. Mater*. **2007**, *6*, 497. (c) Kim, J. Y.; Lee, K.; Coates, N. E.; Moses, D.; Nguyen, T.-Q.; Dante, M.; Heeger, A. J. *Science* **2007**, *317*, 222. (d) Currie, M. J.; Mapel, J. K.; Heidel, T. D.; Goffri, S.; Baldo, M. A. *Science* **2008**, *321*, 226.